

Distributed astrophysics simulations using Octo-Tiger with RISC-V CPUs using HPX and Kokkos

Patrick Diehl^{ID*}§, Gregor Daiß^{ID†}, Steven R. Brandt^{ID*}, Alireza Kheirkhahan^{ID*},
Srinivas Yadav Singanaboina*, Dominic Marcello*,
Chris Taylor^{ID¶}, John Leidel^{ID¶}, and Hartmut Kaiser^{ID*||}

*LSU Center for Computation & Technology, Louisiana State University, Baton Rouge, LA, 70803 U.S.A.

Email: patrickdiehl@lsu.edu

† IPVS, University of Stuttgart, Stuttgart, 70174 Stuttgart, Germany

§ Department of Physics and Astronomy, Louisiana State University, Baton Rouge, LA, 70803 U.S.A.

¶ Tactical Computing Labs, 1001 Pecan St., Lindsay, TX, 776250 U.S.A.

|| Department of Computer Science, Louisiana State University, Baton Rouge, LA, 70803 U.S.A.

Abstract—In recent years, interest in RISC-V computing architectures have moved from academic to mainstream, especially in the field of High Performance Computing where energy limitations are increasingly a point of concern. The results presented in this paper are part of a longer-term evaluation of RISC-V’s viability for HPC applications. In this work, we use the Octo-Tiger multi-physics, multi-scale, 3D adaptive mesh refinement astrophysics application as the bases for our analysis. We report on our experience in porting this modern C++ code (which is built upon several open-source libraries such as HPX and Kokkos) to RISC-V. We also compare the application’s performance, scalability, and power consumption on RISC-V to an A64FX system.

Index Terms—RISC-V, HPX, task-based run time system, asynchronous many-task system, Kokkos

I. INTRODUCTION

RISC-V is an instruction set architecture (ISA) for a general-purpose computer [1]. RISC-V is unique in that, besides its core instructions, the ISA offers a collection of extensions describing different features. The RISC-V extensions are composable, enabling hardware engineers to pick and choose the relevant parts for a desired machine design.

Unlike other ISA efforts, RISC-V’s development is conducted out in the open between hobbyists, academics, and commercial businesses that are working in a competitive market. Competition within the RISC-V community is left to the microarchitecture, hardware implementations of the ISA, and system features (memory, storage, peripherals, etc) offered to consumers.

RISC-V’s status as an open and free ISA has drawn international attention. The European Commission published a study on the impact of Open Source Software and hardware on the European Union’s economy [2], and that included RISC-V. Partly because of this favorable review, the European Union (EU) announced the release of €270 million for building hardware and software based on the RISC-V instruction set.

The European Processor Initiative (EPI)¹ [3] is, perhaps, one of the more important projects for open source, RISC-V, and the development of low-power processors for extreme-scale computing. The project’s ambitious aim is to have the first EU exascale system using RISC-V by 2026. As currently planned, the EU exascale computer will be a CPU only machine without acceleration cards. For these reasons, we decided to compare our RISC-V in-house cluster with supercomputer Fugaku which has Arm A64FX CPUs only.

In addition to the official recognition and promise of future support mentioned above, RISC-V is already making progress toward becoming an HPC technology. Several stable HPC software libraries have been successfully migrated, compiled, and tested using the development boards and single-board computers available so far. The following non-exhaustive list of HPC software has already been successfully migrated and evaluated on RISC-V: Fortran, clang, gcc, OpenMPI, OpenMP, OpenSHMEM, GASNet, UCX, and libfabric.

RISC-V machines up and until 2023 have consisted of IoT and single-board-computers. In December of 2023, a company called MILK-V released the first consumer desktop RISC-V computer, a machine they called “Pioneer.” In contrast to the single-board RISC-V computers, Pioneer features a SOPHON SG2042 RISC-V CPU. The SG2042 is an SoC with 64 cores, 64 MB of cache, and 128 GB of DDR4 on board memory. Previous consumer RISC-V processors have typically offered 4 cores along with 4 or 8 GB on board memory. The Pioneer’s hardware configuration allows, for the first time, the possibility of making a real comparison of RISC-V with other HPC-grade hardware. In this particular case, the HPC-grade hardware is the A64FX nodes of the supercomputer Fugaku. Note that an A64FX node on Fugaku has 48 cores and 28 GB of HBM memory.

This paper is part of an ongoing evaluation of RISC-V’s

¹<https://www.european-processor-initiative.eu/>

viability for HPC applications. Prior work [4] demonstrated that a port of HPX to RISC-V had performance potential to be competitive with A64FX. In the previous paper, we used single-board computers with 4 cores and 8 GB memory. This paper uses a desktop-grade MILK-V Pioneer with a 64-core SOPHON SG2042 RISC-V CPU and 128 GB memory. This allows for larger problem size and a better comparison with the 48 cores of the A64FX CPU. Previously, we added the single-board computer’s CPU as an architecture to Kokko’s CMake build system. For this paper, we had to add the SOPHON SG2042 RISC-V CPU. This paper continues the assessment of RISC-V by providing a focused comparison of a more sophisticated RISC-V machine with A64FX performance using a real-world astrophysics application: the Octo-Tiger HPX application. Octo-tiger is an astrophysics code capable of simulating collisions between stars. Octo-tiger uses a fast-multipole method over adaptive Octrees to evaluate the gravitational potential.

This study has made the following contributions to the HPC software stack:

- Kokkos support for MILK Pioneer’s RISC-V CPU, see pull request #6773².
- Improved HPX support for locks on A64FX, see pull request #6447³. Initially, the target was A64FX, however, improvements on RISC-V were observed as well.
- The first performance study of desktop-grade RISC-V hardware supporting stellar merges using the astrophysics code Octo-Tiger.

The paper is structured as follows: Section II summarizes the related work. The software stack is introduced in Section III. The two scientific applications are briefly discussed in Section IV. The in-house RISC-V cluster is presented in Section V. Node-level and distributed performance results are shown in Section VI. The power consumption is analyzed in Section VII. Finally, the work is concluded in Section VIII.

II. RELATED WORK

Many vendors have provided RISC-V CPUs. A comparison of selected CPUs is available here [4]. Most of these CPUs are development boards, similar to the Raspberry Pi single-board computers for Arm CPUs. RISC-V single-board computers provide a foundation for the development and migration of software to RISC-V. The authors have performed a preliminary study [5] on these single-board computers to port the Octo-Tiger software stack to RISC-V and have completed a scaling study on up to four cores. However, the Milk-V Pioneer’s availability as the first desktop-grade system with 64 Cores creates new opportunities for further testing and evaluation. Milk-V’s Pioneer has been used for a comparison study with x86 CPUs and the *RAJA*Perf benchmarking suite [6] in [7]. A study on software support for academic and industrial applications is available here [8]. The following applications: cryptography [9], deep learning [10], and internet of

things [11] have been explored on RISC-V. However, we are not aware of any study of scientific simulation applications using RISC-V CPUs and AMD GPUs as of the time of this writing.

III. SOFTWARE STACK

In this work, we focus on the performance of our astrophysics application, Octo-Tiger, on RISC-V hardware. In this section, we present its software stack, features, and design decisions to provide a better context for the following results.

Octo-Tiger contains multiple, interleaved solvers (gravity, hydrodynamics and an experimental radiation solver) and uses adaptive mesh refinement (AMR). While the AMR helps with the overall computational load, it makes it difficult to efficiently parallelize and distribute the work onto multiple compute nodes.

In this section, we introduce both Octo-Tiger itself and the software frameworks it employs to alleviate this challenge and provide an efficient distributed implementation with portable compute kernels.

A. HPX

HPX is a distributed, asynchronous many-task runtime system [12]. HPX allows us to express data and execution dependencies by creating a task-graph directly in the source code through the use of futures and continuations. Using this methodology, we can create millions of tasks, all managed by a backend which provides a single worker thread per core. In the context of Octo-Tiger, we use these tasks for asynchronous tree-traversals. One thread can traverse the tree quickly, spawning additional parallel work as it executes, thus avoiding resource starvation.

HPX also provides various features to enable distributed computation: It supports unified syntax and semantics for local and remote operations, asynchronous channels to exchange data, and is implemented for various networking backends (TCP, MPI, LCI [13]). These distributed features work together with HPX futures, allowing us to integrate communication into the task-graph, which, in turn, allows us to finely overlap computation and communication. For Octo-Tiger, this means we do not need to worry about whether a child/parent tree-node is on the same compute node when calling its methods, as HPX takes care of moving the function call to the correct node. These distributed features have been used in the past to run Octo-Tiger on machines such as Piz Daint [14], Summit [15] and, more recently, on the Supercomputer Fugaku [16]. For current runs, we also target Perlmutter.

B. Kokkos and HPX-Kokkos

While HPX can help with the parallelization of the adaptive octree, there is still the issue of computational efficiency within the actual compute kernels that needs to be addressed (as consecutive memory and simple parallel-for patterns would be most efficient on both CPU and GPU).

To address this, Octo-Tiger uses an entire sub-grid within each tree-node for efficiency. This is a tradeoff, hurting the

²<https://github.com/kokkos/kokkos/pull/6773>

³<https://github.com/STELLAR-GROUP/hpx/pull/6447>

adaptivity, and therefore we usually limit the sub-grid size to $8x8x8$ (though this is adjustable at compile time). Together with a ghost-layer for each sub-grid, these $8x8x8$ cells are the input for the actual compute kernels in the gravity and hydro solver.

This already eases the kernel development as the compute kernels deal with a regular, albeit small, data-structure. However, we still need to target various hardware platforms (as Octo-Tiger targets both CPU and GPU supercomputers).

In order to address portability concerns, we use Kokkos. Kokkos is a performance portability framework, originally developed at Sandia National Laboratories [17]. Kokkos offers multiple hardware abstractions in the form of memory and execution spaces. Using Kokkos means we only have to develop each compute kernel once. Compute kernels are instantiated at compile time with the correct memory and execution space for the given hardware (for instance the Kokkos CUDA spaces for NVIDIA hardware).

In order to increase efficiency on CPU platforms, SIMD data-types support is available. SIMD data-types instantiate to scalar data-types on the GPU ensuring the kernel implementation stays compatible with GPUs. On an x86 machine, SIMD data-types instantiate to AVX512 types along with the appropriate AVX512 instructions.

Furthermore, Kokkos is well integrated with HPX.

First, there is the HPX execution space [18]: This space allows users to execute a Kokkos kernel with HPX worker threads (eliminating the need for any conflicting thread pools that would occur when using the Kokkos OpenMP execution space).

Second, there is the HPX-Kokkos compatibility layer: It allows programmers to make asynchronous Kokkos calls for most execution and memory spaces (works with the HPX, CUDA, HIP and SYCL spaces [19] spaces). This allows direct integration of Kokkos kernels into the HPX task graph.

Currently, all major compute kernels in the HPX hydro and gravity solver have been ported to Kokkos. We use additional techniques to increase the efficiency given our specific use-case within Octo-Tiger: kernel fusion for the kernels on larger GPUs [20] (as the $8x8x8$ proved to be too much a bottleneck here otherwise, starving the GPU), and on A64Fx we had issues with the SVE SIMD types and ended up using our own (std :: experimental :: simd-compatible SVE types within the Kokkos kernels [21]).

C. Octo-Tiger

Octo-Tiger is a specialized code designed to model self-gravitating astrophysical fluids, particularly focusing on interacting binary systems [22]. Utilizing a combination of techniques, Octo-Tiger offers a comprehensive approach to understanding these complex astrophysical phenomena.

Octo-Tiger leverages several key features to accurately model interacting binary systems. Employing the finite volume method enables calculations of fluid dynamics. Octo-Tiger incorporates a rotating grid, aligning the frame of reference with the binary system’s initial orbital period, reducing effects

of numerical viscosity. Gravity modeling is facilitated through the Fast Multipole Method (FMM). Notably, the FMM conserves both linear and angular momentum, distinguishing it from conventional FMM approaches and enhancing simulation accuracy by enabling machine precision energy conservation within the rotating frame. Adaptive Mesh Refinement (AMR) techniques dynamically adjust computational grid resolution, allowing for efficient resource allocation by concentrating computational power where it is most necessary. Octo-Tiger evolves the system forward in time using the method of lines coupled with a third or Runge Kutta integrator. Additionally, Octo-Tiger’s optimization for various architectures ensures that researchers can leverage its capabilities across diverse hardware platforms.

Due to its high optimization and the faster convergence of the finite volume method compared to smoothed particle hydrodynamics (SPH), Octo-Tiger has proven to be valuable for convergence studies (e.g. [23], [24]). These studies involve employing progressively finer resolutions on the same model to distinguish physical effects from numerical artifacts.

IV. SCIENTIFIC APPLICATIONS

Having introduced Octo-Tiger, its software stack, and its features in the last section, we now take a look at the current research questions (beyond mere performance studies) for which Octo-Tiger is actively being used. Notably, we use some of these production simulations (for just a few time-steps at a low resolution) to generate the performance comparisons later on. Hence, we focus on the viability of the RISC-V hardware not for some synthetic benchmarks, but rather for real-world production scenarios.

A. Double White Dwarf Systems

A double white dwarf (DWD) system consists of two compact stellar remnants, each having exhausted its nuclear fuel and collapsed to a dense, Earth-sized object. Over time, gravitational wave emission causes the orbital separation to decrease. If this becomes small enough, mass can be pulled from one white dwarf, the “donor”, to the other, the “accretor”, and in many cases this interaction is unstable, leading to runaway mass transfer and merger.

The potential for a Type Ia supernova arises if their combined mass exceeds $1.4 M_{\odot}$. Conversely, if the interaction results in a merger with a combined mass below this threshold, it can lead to the formation of an intriguing celestial object known as R Coronae Borealis star (RCB). RCB stars are characterized by their peculiar elemental abundances, notably low to non-existent hydrogen content. Since white dwarfs are what is leftover after a star uses all of its hydrogen fuel, this suggests DWDs as a formation channel. While Octo-Tiger cannot model thermonuclear explosions like Type Ia supernova, it serves as a valuable tool for studying RCB formation. In particular, it can be used to study the dredge up of elements such as Oxygen-16 from the cores of the accretor to the surface of the RCB star during merger. We use restart files from production runs close to the merger [23] where

adaptive mesh refinement happened as one of our tests. In this case, the mesh is very unbalanced and shows characteristics of a production run.

We will run two types of tests using a double white dwarf: DWD Separated and DWD Merging. The former corresponds to the beginning of a typical scientific simulation. At this point, the grids are fairly regular and balanced and we run it for 10 time steps. The latter corresponds to a checkpoint restart from a time very near the merging of the two stars. At this point, the grids have had time to dynamically reshape themselves to the physics and are far less regular and balanced. We run this one for 20 time steps.

B. v1309

In contact binary systems, two stars orbit so closely that they share a common envelope of gas. As one or both stars evolve, they may reach a critical point where one star expands and engulfs its companion. This process can culminate in a luminous red nova (LRN), characterized by a sudden surge in brightness and the ejection of material.

One notable example of such an event occurred in September 2008 when the contact binary star system V1309 Sco underwent a merger [25]. The system’s brightness increased by a factor of approximately one hundred. What made the observation of V1309 Sco remarkable was the extensive pre-merger data collected by the Optical Gravitational Lensing Experiment (OGLE). For six years leading up to the merger, OGLE meticulously documented the system’s behavior, providing a rare opportunity to observe a stellar merger both before and after the event.

One goal of Octo-Tiger is to be able to model the light curve generated by merger events like V1309 Sco. This requires careful treatment of the transition between the optically thick and optically thin regions in the stellar atmosphere. Octo-Tiger is able to add extra resolution to the stellar atmosphere, providing a more accurate representation of the transition region. Octo-Tiger also has a specialized implementation of the self consistent field (SCF) module used to generate initial conditions for binary stars [26]. This version is able to produce models with common atmospheres, like the progenitor of V1309 Sco. We have included a model of V1309 Sco in this paper. This model does not include the effects of radiation transport, since this module of Octo-Tiger had not been developed at the time it was produced.

This test tends to be quite memory intensive and we run it for 10 time steps.

V. IN-HOUSE RISC-V CLUSTER

For this paper, we built an in-house cluster with two nodes. Each node is a Milk-V Pioneer desktop machine with a 64-core SOPHON SG2042 RISC-V CPU, 128 GB DDR4 RAM, and a 1TB PCI 3.0 SSD card. The nodes are connected via Ethernet using Intel X540-T2 network cards. Figure 1 shows an image of one of the nodes. We named the cluster Olaf ☺ after the snowman from the movie Frozen, since the color scheme reminded us of that character.



Fig. 1: Image of one of the MILK-V Pioneer nodes of the in-house cluster. Each node has a 64-core SOPHON SG2042 RISC-V CPU and 128 GB DDR4 System Memory. The colorscheme of box (the orange handle and white case) reminded us of the snowman Olaf from the movie Frozen. For this reason, we named the cluster Olaf ☺.

The machine comes with *Fedora 38* preinstalled. The original disk partition occupied only a fraction of the NVMe disk, so we expanded it. After that, it was easy to install additional packages with *dnf*. The default *slurm* provided by the repository was sufficient to create a cluster from the two nodes. The system applications were installed on the local disk, the libraries and the test application as well as users’ home directories were hosted by an NFS shared file system. We were not able to upgrade the Linux kernel provided by the repository, all attempts resulted in error messages that the new kernel is in conflict with installed kernel. Setting aside the kernel upgrade issue, the current kernel worked perfectly for our test environment. It should be noted that the need for security updates will require administrators to find a way to upgrade the Linux kernel.

VI. PERFORMANCE RESULTS

In this section, we present node-level scaling for the Mandelbrot set for various types of shared memory parallelism in HPX, see Section VI-A. In addition, we show node-level scaling for the astrophysics application Octo-Tiger using the rotating star test problem and the double white dwarf (DWD) real-world scenarios described in Section VI-B. In Section VI-C, we show distributed results using two real-world scenarios, namely DWD and v1309. Table I shows the compiler and software versions used in this paper on the RISC-V cluster.

TABLE I: Compiler and software versions used to build Octo-Tiger with CMake 3.19.5. We optimized HPX for RISC-V and A64FX and used a specific commit of HPX’s development branch for some of the runs.

gcc	HPX	Boost	openmpi	hwloc
13.2.1	72ca840/1.9.1	1.84	4.1.2	1.11.12
Kokkos 4.0.01	HPX-Kokkos 0.4.0	cppuddle c084385	jemalloc 5.2.1	Octo-Tiger dd5cb880

A. HPX benchmarks

The first Mandelbrot set was computed and visualized in 1978 [27]. The figure is computed from Equation (1) and parallelized in three ways: using parallel algorithms, using futures and coroutines, and using senders & receivers. We refer to a previous publication [28] for implementation details. The code is available on GitHub [29].

$$z_{n+1} = z_n^2 + c. \quad (1)$$

Figure 2 shows the pixels updated per second for all approaches. For all three parallelization approaches, Intel and AMD have comparable performance. Note the runs on A64FX were done on Stony Brook’s Ookami cluster. The Ookami cluster has the same A64FX CPU as in supercomputer Fugaku. However, Ookami uses Infiniband as the network layer and supercomputer Fugaku uses Tofu-D. However, since we are doing single-node runs the different network layers is not important for performance. The performance on A64FX is around three times slower for all approaches. For futures and coroutines (See Figure 2a) the performance on A64FX is slightly better than on RISC-V. With the C++ 20 standard, coroutines were added. In HPX, coroutines can be combined with futures to simplify continuations. Figure 2b shows the combination of coroutines and futures. For the parallel algorithm in Figure 2c, the performance on A64FX is comparable with RISC-V. Figure 2d shows the results using the experimental feature of senders and receivers in HPX. HPX implements the latest draft of P2300⁴ which might be included in the upcoming C++ 26 standard. Here, RISC-V is slightly faster than A64FX. Since the performance of A64FX and RISC-V is similar, we will only compare against A64FX for all further runs.

B. Node-level scaling (Octo-Tiger)

1) *Rotating star*: We use the single rotating star example from Octo-Tiger’s test suite. Figure 3 shows the scaling for the level of refinement 5 with an octree containing 2,220 leaves and 2,584,576 cells.

We ran this scenario on a single MILK-V board with 64 cores in total and on a single Supercomputer Fugaku node with 48 cores. For simulations using 8 cores or less, A64FX was faster. At higher core counts, the RISC-V cpu (black lines) was faster. We investigated the poor performance on A64FX

TABLE II: Average floating point operations (FLOP) per timestep, Number of cells, the memory usage, and the file size of the input file for all three refinement levels.

Level	FLOP	# cells	Memory	File size
10 (initial)	5.28×10^{11}	1.6M	5 GB	72MB
10 (refined)	1.68×10^{12}	3.8M	11 GB	548MB
11 (initial)	1.11×10^{12}	3.6M	10 GB	162MB
11 (refined)	1.75×10^{13}	40.2M	113 GB	5.8 GB

and discovered that 128 bit atomics were actually simulated using locks on both A64FX and RISC-V by the C++ standard lib. This had a significant impact on performance because HPX uses 128 bit atomics in its internal scheduling and synchronization. An alternate solution for the schedulers is to use 64-bit atomics, which are lock-free on both A64FX and RISC-V. The 64 bit atomics are enabled for HPX scheduler’s by configuring HPX_LOCKFREE_PTR_COMPRESSION=ON when invoking cmake, see pull request # 6447³.

We executed the same test using the same dependencies, except for a newer HPX version with the optimization (gray lines). After optimizing, the performance of A64FX and RISC-V are almost identical (but now reversed, with A64FX being slightly faster above 8 cores).

2) *DWD*: This section uses the mesh from some recent production runs for a double white dwarf (DWD) merger. We use real-world production runs and initial data for these tests. In particular, we ran DWD Separated (where the stars are widely separated), and DWD Merging (which uses restart files to follow a nearly complete simulation) and ran with both 10 and 11 levels of adaptive mesh refinement [23]. Table II shows the average floating point operations measured using the *perf* tool on an Intel Skylake CPU.

Figure 4a shows the scaling for both runs. With 10 levels of refinement, the code has higher throughput because there are fewer cells. Both levels scale well on the single node. The gray line shows the runs that use atomics instead of locks. We see a significant improvement in this case for runs with 11 levels of refinement, but still see some improvement for 10 levels of refinement (but only for higher core counts). Figure 4b shows the DWD Merging experiment with 10 and 11 levels of refinement.

C. Distributed scaling (Octo-Tiger)

1) *DWD*: First, we executed the runs for the node-level scaling in the previous section using all 64 cores per node on two nodes. Figure 5 shows the results for level 10. For the DWD Separated in Figure 5a, we observe some improvements, however, the workload was not large enough. For the DWD Merging case in Figure 5b, the workload was sufficient and we observed a better improvement. For all node counts the A64FX runs were slower. However, we have to take into account that an A64FX node has 48 cores and a RISC-V core has 64 cores.

Figure 6 shows the results for the DWD Separated of Level 11. Here, on the single node both runs are comparable. However, on two nodes the RISC-V run is slightly faster.

⁴<https://en.cppreference.com/w/cpp/experimental/execution>

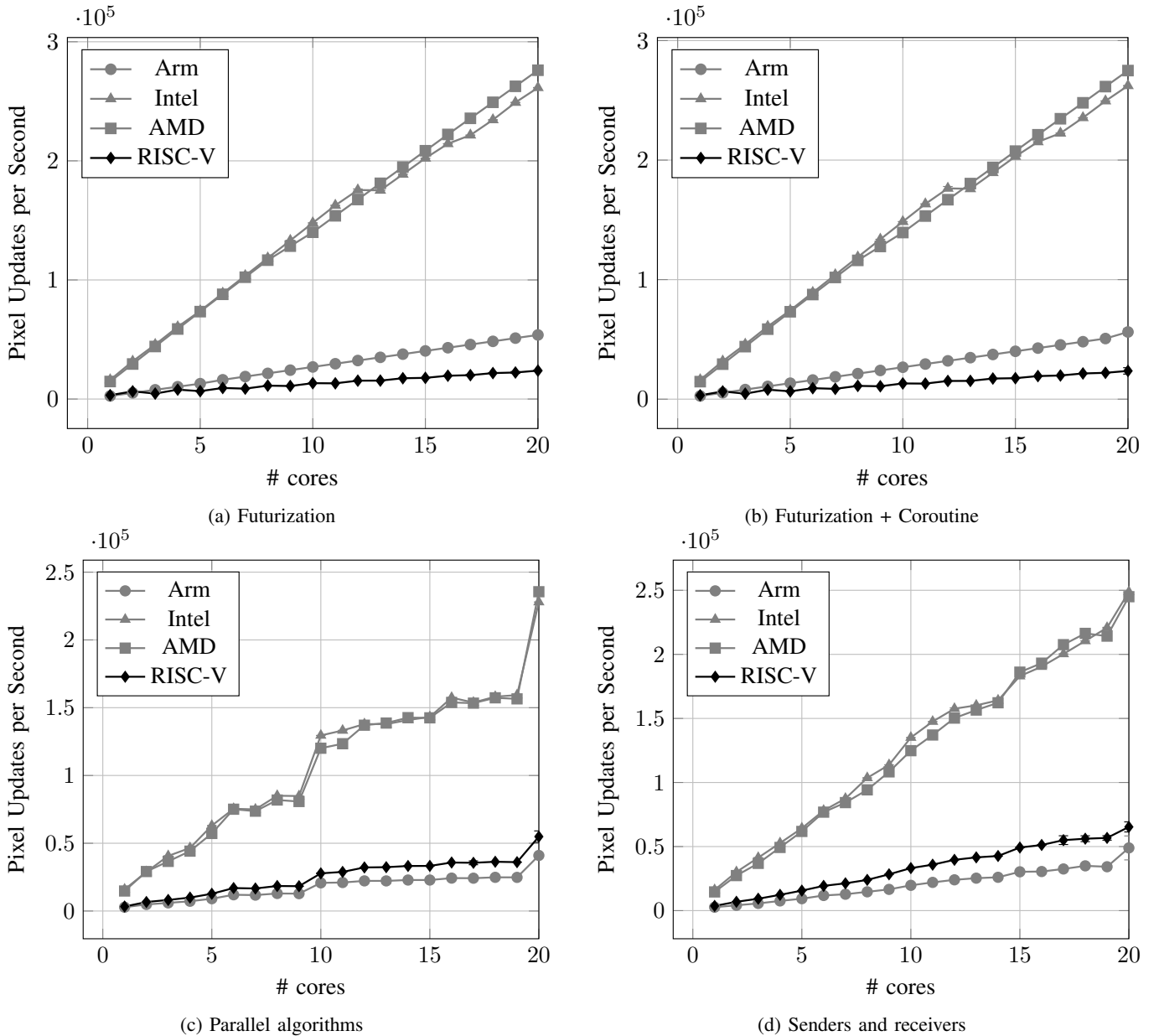


Fig. 2: The median out of ten runs using different methods for parallelizing the Mandelbrot set. Using `hpx::future` (a), `future + coroutine` (b), HPX’s parallel algorithms using `hpx::for_loop` (c), and senders and receivers (d). We computed the Mandelbrot set in Equation (1) for $20,000 \times 20,000$ pixels to create an artificial work load. The data for Arm, Intel, and AMD was taken from [28].

However, we must consider that an A64FX node has 48 cores and a RISC-V core has 64. Table III shows the MFLOP/s for all levels.

2) *V1309*: In this section, we look into the scaling of the production run of the *v1309* scenario. Here, we ran the code for 10 time steps. Figure 7 shows the distributed scaling. Here, due to the restricted limit of 28 GB of memory per node, we had to use 16 Supercomputer Fugaku nodes. We experienced similar issues with less memory on Supercomputer Fugaku while comparing with NERSC’S Perlmutter [30]. We observe that we get around 100 more sub-grids per second processed

on RISC-V using a single node as for 16 supercomputer Fugaku nodes.

VII. POWER MEASUREMENTS

We compared the RISC-V boards and Supercomputer Fugaku for both scenarios. For the Sophon RISC-V CPU, no hardware counters are available. For the single-board computers, we attached a USB power meter to approximate the power consumption [4]. However, the desktop computer has a regular connector for regular sockets. The manufacturer reports

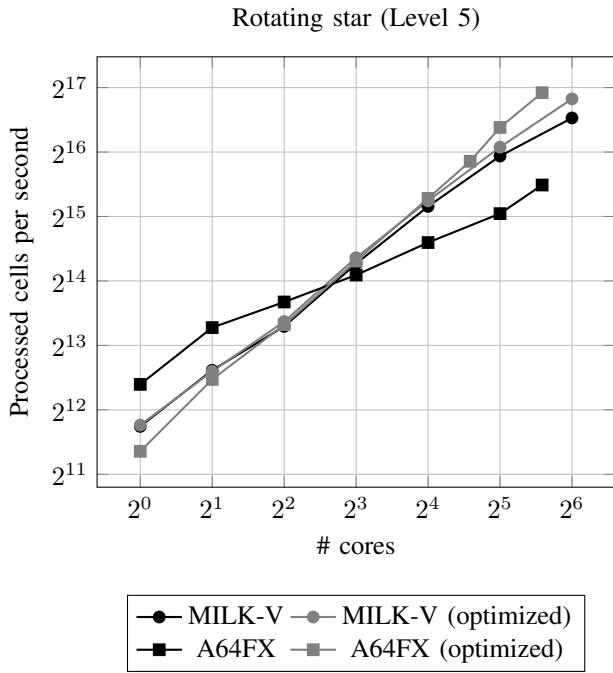


Fig. 3: Single node scaling for a rotating star on ARM A64FX and RISC-V.

TABLE III: MFLOP per time step for single node and two node runs on RISC-V and A64FX. Note that a RISC-V node has 64 cores and a A64FX code has 48 cores.

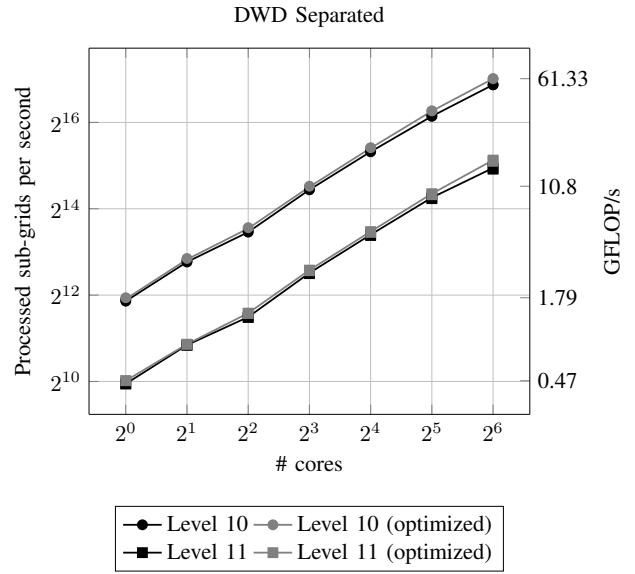
Level	1 node		2 nodes	
	RISC-V	A64FX	RISC-V	A64FX
10 (initial)	153.34	93.56	196.68	105.86
10 (refined)	148.87	88.11	248.57	113.43
11 (initial)	161.58	73.97	261.67	101.77

a typical power consumption of 120 watts⁵. The typical power consumption of one supercomputer Fugaku node is around 200 Watts [31].

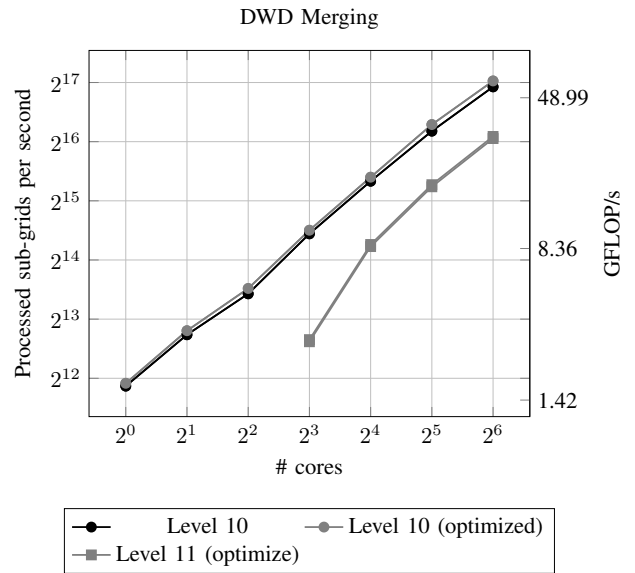
1) *DWD*: Figure 8 shows the power consumption for both meshes of level 10. Here, RISC-V has around two times less power consumption on a single node and three times less on two nodes.

Figure 9 shows the power consumption for the DWD Separated of level 11. Here, both architectures have a similar power consumption. Note that on supercomputer Fugaku Sandia’s PowerAPI [32] is integrated with the PJM job scheduler. Thus, for all runs, information about the power consumption is available. For the used RISC-V CPU, no hardware counters or software tools are available yet. For future comparison, it would be beneficial to obtain a more accurate power consumption measurement on RISC-V. For a fair comparison in this paper, we used the typical energy consumption for a single node provided by the manufacturer.

⁵<https://milkv.io/pioneer>



(a)



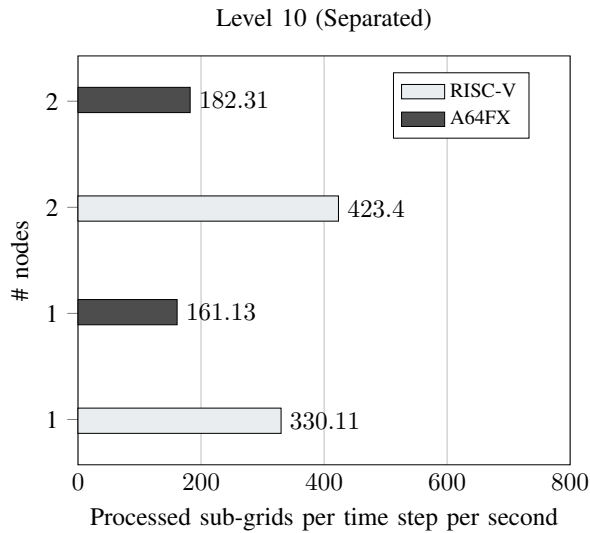
(b)

Fig. 4: Single node scaling for a DWD Separated and b DWD Merging, respectively. For DWD Merging with 11 levels, we only used the optimized code. **The run on 8 cores took around 34 hours and we skipped the runs on 4 cores, 2 cores, and a single core since these runs were not feasible.**

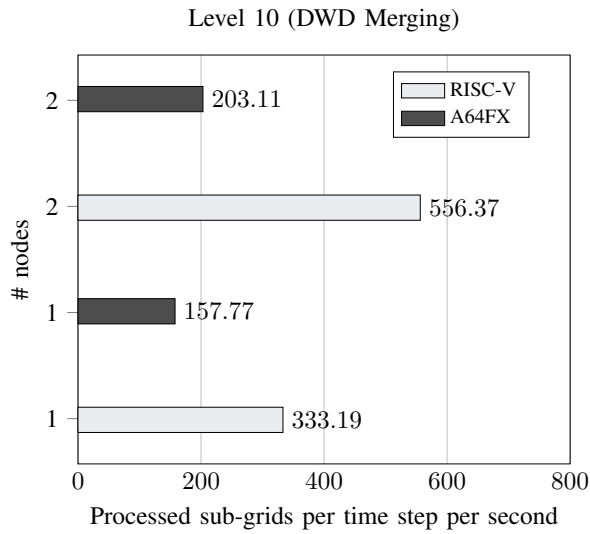
2) *V1309*: Figure 10 shows the power consumption for a single time step of the v1309 scenario. The scenario fitted in one RISC-V node. Due to the 28 GB memory of the supercomputer Fugaku nodes, we had to use 16 nodes. The power consumption is around 50% higher on A64FX.

VIII. CONCLUSION

The Pioneer RISC-V machines used in this paper are the first desktop-grade systems available for general use. While most of the porting of the HPX to RISC-V was done in the



(a)



(b)

Fig. 5: Distributed scaling for a single node and two nodes using MPI for communication on RISC-V and Supercomputer Fugaku. Unfortunately, our in-house cluster only had two nodes. Note that we used all cores of the nodes. Recall that an A64FX node has 48 cores and a RISC-V node has 64 cores.

author’s previous work [5], this study required optimizations for HPX’s atomic support for Arm and RISC-V. In addition, changes were made to Kokko’s CMake build system in order to support the Pioneer’s RISC-V Sophon CPU. Modifications to Kokko’s CMake system brought to the forefront questions about how to handle different flavors of RISC-V processors in the Kokkos build system moving forward.

Previously, we compared Octo-Tiger’s performance on single-board computers with 4 cores and memory controllers which did not meet the expectations for HPC-grade hardware. Now, with 64 cores and faster memory controllers, larger scenarios can be investigated. For the rotating star scenario,

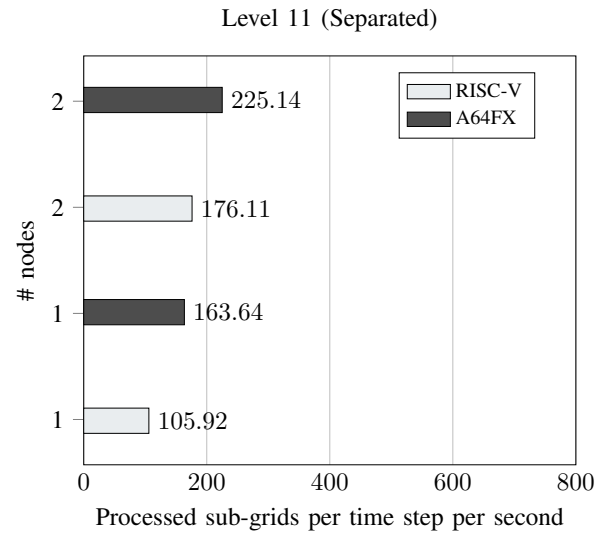


Fig. 6: Distributed scaling for a single node and two nodes using MPI for communication on RISC-V and Supercomputer Fugaku. Unfortunately, our in-house cluster only had two nodes. Note that we used all cores of the nodes. Recall that an A64FX node has 48 cores and a RISC-V node has 64 cores.

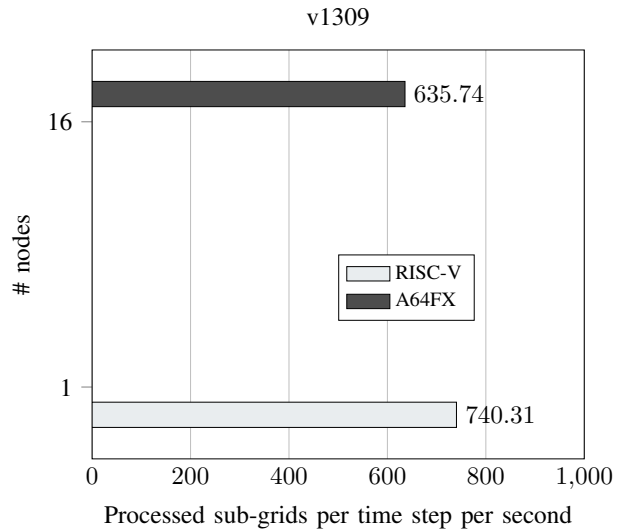
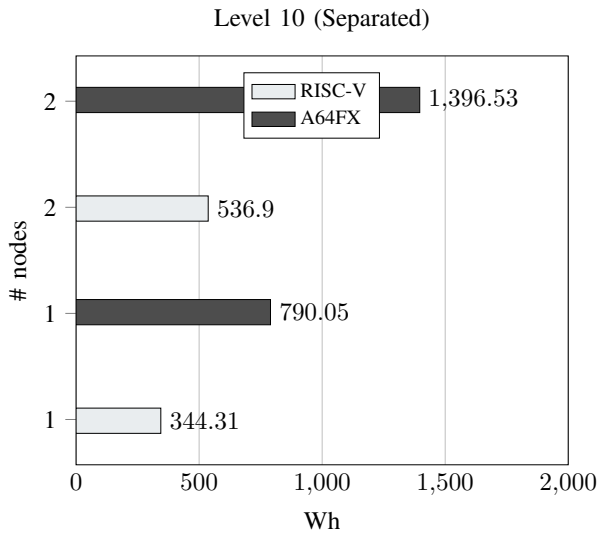
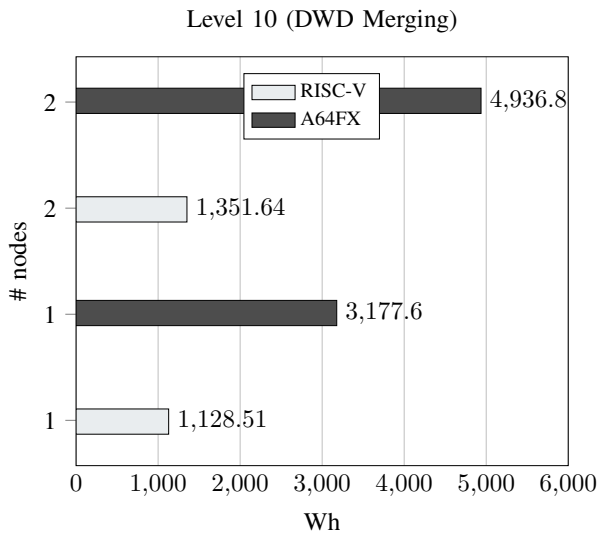


Fig. 7: Processed sub-grids for a single time step for the v1309 scenario. The v1309 scenario fitted in a single RISC-V node with 128 GB memory. Due to the 28 GB memory per supercomputer Fugaku node, we had to use 16 nodes. So we used 64 RISC-V cores on a single node and 769 A64FX cores on 16 nodes with 48 cores per node.

A64FX and RISC-V showed comparable performance with the improved HPX support for atomics on A64FX. The improved atomics showed improvements on RISC-V for larger scenarios too. We observed scaling from a single core up to 64 cores on RISC-V for the node-level runs. For a detailed node-level performance analysis on A64FX for Ookami and supercomputer Fugaku, we refer to [16].



(a)



(b)

Fig. 8: Power consumption for a single node and two nodes using MPI for communication on RISC-V and Supercomputer Fugaku. Unfortunately, our in-house cluster only had two nodes. Note that we used all cores of the nodes. Recall that an A64FX node has 48 cores and a RISC-V node has 64 cores.

For the first scenario, the double white dwarf (DWD), we compared the sub-grids processed per time step per second and the floating point operations per time step on a single node and two nodes. In most cases, the RISC-V nodes were slightly faster. One reason for the performance difference can be attributed to the A64FX nodes have 48 cores and the RISC-V nodes have 64 cores. For the second scenario, the v1309, the input file was much larger and the scenario did not fit into a single A64FX node due to the 28 GB memory limit per node. Instead, 16 nodes were required. Here, we got comparable sub-grids processed per time step per second. Using the desktop-grade RISC-V hardware resulted in similar

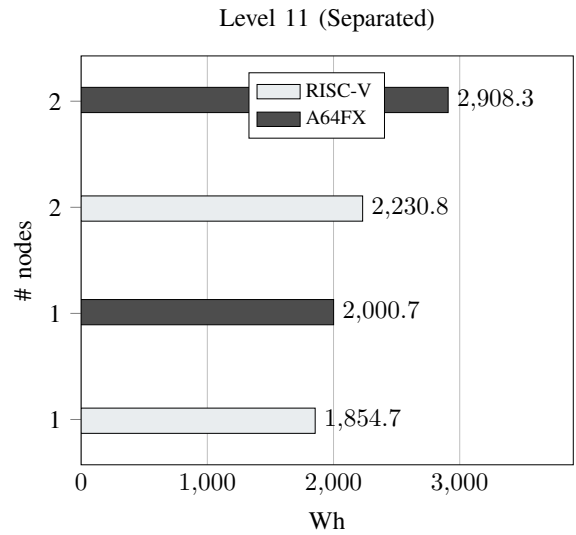


Fig. 9: Power consumption for a single node and two nodes using MPI for communication on RISC-V and Supercomputer Fugaku. Unfortunately, our in-house cluster only had two nodes. Note that we used all cores of the nodes. Recall that an A64FX node has 48 cores and a RISC-V node has 64 cores.

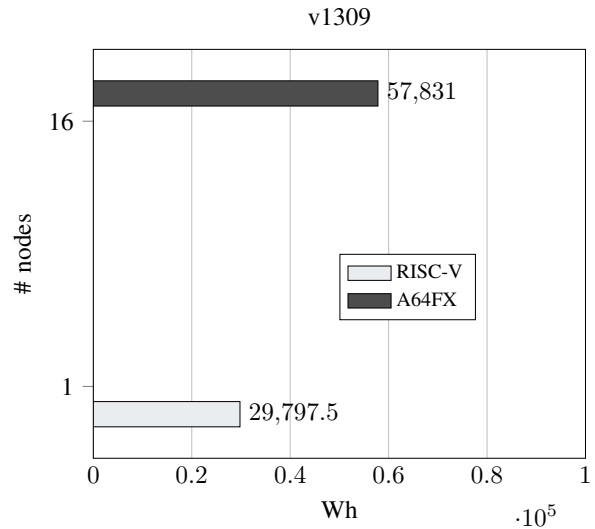


Fig. 10: Power consumption for a single time step for the v1309 scenario. The v1309 scenario was able to fit in a single RISC-V node with 128 GB memory. Due to the 28 GB memory per supercomputer Fugaku node, we had to use 16 nodes. So we used 64 RISC-V cores on a single node and 769 A64FX cores on 16 nodes with 48 cores per node.

performance concerning A64FX taking the core difference into account.

When considering power consumption, we observed the RISC-V system generally used less energy for some runs. The typical energy consumption of a RISC-V node is 120 Watts, and for a supercomputer Fugaku node is 200 Watts [31]. In a couple of instances, however, both architectures shared

comparable power utilization.

Octo-Tiger supports GPU's via Kokkos. We believe a follow up study of heterogeneous computations using RISC-V CPUs and GPUs is supported by this work. As of this writing, there are no CUDA drivers or NVIDIA SDK for RISC-V. AMD's latest consumer GPUs work on RISC-V platforms. In light of AMD's support for RISC-V, a follow up study investigating Kokkos kernel execution on a heterogeneous system with an AMD GPU and RISC-V CPU is worth pursuing. All the steps in our study are in preparation for the European Processor Initiative (EPI). The European Union has recently announced a substantial investment towards the development of HPC RISC-V hardware and software. These efforts are pivotal in laying the groundwork for the eventual deployment of the RISC-V-based European supercomputer slated for launch in 2026.

Overall, this work demonstrates the viability of current RISC-V hardware generation for real-world astrophysics simulations. Notably, we encountered no significant issues running Octo-Tiger on this first-gen RISC-V desktop hardware. Even given Octo-Tiger's somewhat unusual software stack (using HPX over MPI+OpenMP), production-grade simulations easily scaled to all cores and multiple nodes on this novel hardware platform.

Overall, our experiences gives us cautious optimism regarding the platform itself. We plan to repeat this benchmark once newer RISC-V (server-grade) platforms are available. Looking toward to future RISC-V studies, several vendors and opportunities are on the horizon. We look forward to assessing Octo-Tiger's performance on the following RISC-V architectures: Ventana's Veyron V2, X-Silicon's C-GPU, and Tenstorrent's Ascalon. Since the European RISC-V supercomputer will be a CPU-only machine, we have focused on the comparison with supercomputer Fugaku which is also a CPU-only machine.

The following features added to the RISC-V ISA would be beneficial for asynchronous many-task runtime systems like HPX: one-cycle context switches, extended atomics, hardware support for global address space, and hardware support for thread scheduling (hardware queues). For general HPC workloads the RISC-V vector machine extension, user-land cache management and control, and hardware counters for power consumption would be beneficial.

ACKNOWLEDGMENT

This research employed computational resources of the supercomputer Fugaku provided by RIKEN Center for Computational Science. We thank the LSU Center of Computation & Technology for supporting this work. The authors would like to thank Stony Brook Research Computing and Cyberinfrastructure, and the Institute for Advanced Computational Science at Stony Brook University for access to the innovative high-performance Ookami computing system, which was made possible by a \$5M National Science Foundation grant (#1927880).

SUPPLEMENTARY MATERIALS

The build scripts to build Octo-Tiger and all its dependencies are available on GitHub⁶. Octo-Tiger⁷, HPX⁸, and HPX-Kokkos⁹ are available on GitHub. The input files for the v1309 scenario are available on Zenodo [33]. The DWD scenarios are available upon request, as an astrophysics paper [23] is under preparation. The slurm job scripts and specific input data are available on GitHub¹⁰.

REFERENCES

- [1] A. Waterman, Y. Lee, D. Patterson, K. Asanovic, V. I. U. level Isa, A. Waterman, Y. Lee, and D. Patterson, "The RISC-V instruction set manual," *Volume 1: User-Level ISA*, version, vol. 2, pp. 1–79, 2014.
- [2] K. Blind, M. Böhm, P. Grzegorzewska, A. Katz, S. Muto, S. Patsch, and T. Schubert, "The impact of Open Source Software and Hardware on technological independence, competitiveness and innovation in the EU economy," *Final Study Report. European Commission, Brussels*, doi, vol. 10, p. 430161, 2021.
- [3] M. Kovač *et al.*, "European processor initiative (EPI)—An approach for a future automotive eHPC semiconductor platform," in *Electronic Components and Systems for Automotive Applications: Proceedings of the 5th CESA Automotive Electronics Congress, Paris, 2018*. Springer, 2019, pp. 185–195.
- [4] A. Dörflinger *et al.*, "A Comparative Survey of Open-Source Application-Class RISC-V Processor Implementations," in *Proceedings of the 18th ACM International Conference on Computing Frontiers*, ser. CF '21. New York, NY, USA: Association for Computing Machinery, 2021, p. 12–20. [Online]. Available: <https://doi.org/10.1145/3457388.3458657>
- [5] P. Diehl, G. Daiss, S. Brandt, A. Kheirkhahan, H. Kaiser, C. Taylor, and J. Leidel, "Evaluating HPX and Kokkos on RISC-V using an astrophysics application Octo-Tiger," in *Proceedings of The International Conference on High Performance Computing, Network, Storage, and Analysis*, 2023, pp. 1533–1542.
- [6] R. D. Hornung and H. E. Hones, "Raja performance suite," Lawrence Livermore National Lab.(LLNL), Livermore, CA (United States), Tech. Rep., 2017.
- [7] N. Brown, M. Jamieson, J. Lee, and P. Wang, "Is RISC-V ready for HPC prime-time: Evaluating the 64-core Sophon SG2042 RISC-V CPU," in *Proceedings of the SC '23 Workshops of The International Conference on High Performance Computing, Network, Storage, and Analysis*, ser. SC-W '23. New York, NY, USA: Association for Computing Machinery, 2023, p. 1566–1574. [Online]. Available: <https://doi.org/10.1145/3624062.3624234>
- [8] B. W. Mezger, D. A. Santos, L. Diliillo, C. A. Zeferino, and D. R. Melo, "A Survey of the RISC-V Architecture Software Support," *IEEE Access*, vol. 10, pp. 51 394–51 411, 2022.
- [9] K. Stoffelen, "Efficient cryptography on the RISC-V architecture," in *Progress in Cryptology—LATINCRYPT 2019: 6th International Conference on Cryptology and Information Security in Latin America, Santiago de Chile, Chile, October 2–4, 2019, Proceedings 6*, Springer. Santiago de Chile, Chile: Springer, 2019, pp. 323–340.
- [10] M. S. Louis *et al.*, "Towards deep learning using tensorflow lite on RISC-V," in *Third Workshop on Computer Architecture Research with RISC-V (CARRV)*, vol. 1. Phoenix, Arizona: ACM, 2019, p. 6.
- [11] P. D. Schiavone *et al.*, "Slow and steady wins the race? A comparison of ultra-low-power RISC-V cores for Internet-of-Things applications," in *2017 27th International Symposium on Power and Timing Modeling, Optimization and Simulation (PATMOS)*, IEEE. Thessaloniki, Greece: IEEE, 2017, pp. 1–8.

⁶<https://github.com/STELLAR-GROUP/OctoTigerBuildChain>

⁷<https://github.com/STELLAR-GROUP/octotiger>

⁸<https://github.com/STELLAR-GROUP/hpx>

⁹<https://github.com/STELLAR-GROUP/hpx-kokkos>

¹⁰<https://github.com/diehlpapers/RISC-V-24>

- [12] H. Kaiser, P. Diehl, A. S. Lemoine, B. A. Lelbach, P. Amini, A. Berge, J. Biddiscombe, S. R. Brandt, N. Gupta, T. Heller, K. Huck, Z. Khatami, A. Kheirkhan, A. Reverdell, S. Shirzad, M. Simberg, B. Wagle, W. Wei, and T. Zhang, "HPX - The C++ Standard Library for Parallelism and Concurrency," *Journal of Open Source Software*, vol. 5, no. 53, p. 2352, 2020. [Online]. Available: <https://doi.org/10.21105/joss.02352>
- [13] J. Yan, H. Kaiser, and M. Snir, "Design and Analysis of the Network Software Stack of an Asynchronous Many-task System – The LCI parcelport of HPX," in *Proceedings of the SC '23 Workshops of The International Conference on High Performance Computing, Network, Storage, and Analysis*, ser. SC-W '23. New York, NY, USA: Association for Computing Machinery, 2023, p. 1151–1161. [Online]. Available: <https://doi.org/10.1145/3624062.3624598>
- [14] G. Daiß *et al.*, "From Piz Daint to the Stars: Simulation of Stellar Mergers Using High-Level Abstractions," in *Proceedings of the International Conference for High Performance Computing, Networking, Storage and Analysis*, ser. SC '19. New York, NY, USA: Association for Computing Machinery, 2019. [Online]. Available: <https://doi.org/10.1145/3295500.3356221>
- [15] P. Diehl, G. Daiß, D. Marcelllo, K. Huck, S. Shiber, H. Kaiser, J. Frank, G. C. Clayton, and D. Pflüger, "Octo-Tiger's New Hydro Module and Performance Using HPX+CUDA on ORNL's Summit," in *2021 IEEE International Conference on Cluster Computing (CLUSTER)*, 2021, pp. 204–214.
- [16] P. Diehl, G. Daiß, K. Huck, D. Marcelllo, S. Shiber, H. Kaiser, and D. Pflüger, "Simulating stellar merger using HPX/Kokkos on A64FX on Supercomputer Fugaku," *The Journal of Supercomputing*, 2024. [Online]. Available: <https://doi.org/10.1007/s11227-024-06113-w>
- [17] C. R. Trott, D. Lebrun-Grandié, D. Arndt, J. Ciesko, V. Dang, N. Ellingwood, R. Gayatri, E. Harvey, D. S. Hollman, D. Ibanez, N. Liber, J. Madson, J. Miles, D. Poliakoff, A. Powell, S. Rajamanickam, M. Simberg, D. Sunderland, B. Turcksin, and J. Wilke, "Kokkos 3: Programming Model Extensions for the Exascale Era," *IEEE Transactions on Parallel and Distributed Systems*, vol. 33, no. 4, pp. 805–817, 2022.
- [18] G. Daiß, M. Simberg, A. Reverdell, J. Biddiscombe, T. Pollinger, H. Kaiser, and D. Pflüger, "Beyond Fork-Join: Integration of Performance Portable Kokkos Kernels with HPX," in *2021 IEEE International Parallel and Distributed Processing Symposium Workshops (IPDPSW)*, 2021, pp. 377–386.
- [19] G. Daiß, P. Diehl, H. Kaiser, and D. Pflüger, "Stellar Mergers with HPX-Kokkos and SYCL: Methods of Using an Asynchronous Many-Task Runtime System with SYCL," in *Proceedings of the 2023 International Workshop on OpenCL*, ser. IWOCCL '23. New York, NY, USA: Association for Computing Machinery, 2023. [Online]. Available: <https://doi.org/10.1145/3585341.3585354>
- [20] G. Daiß, P. Diehl, D. Marcelllo, A. Kheirkhan, H. Kaiser, and D. Pflüger, "From Task-Based GPU Work Aggregation to Stellar Mergers: Turning Fine-Grained CPU Tasks into Portable GPU Kernels," in *2022 IEEE/ACM International Workshop on Performance, Portability and Productivity in HPC (P3HPC)*. Los Alamitos, CA, USA: IEEE Computer Society, nov 2022, pp. 89–99. [Online]. Available: <https://doi.ieeecomputersociety.org/10.1109/P3HPC56579.2022.00014>
- [21] G. Daiß, S. Singanaboina, P. Diehl, H. Kaiser, and D. Pflüger, "From Merging Frameworks to Merging Stars: Experiences using HPX, Kokkos and SIMD Types," in *2022 IEEE/ACM 7th International Workshop on Extreme Scale Programming Models and Middleware (ESPM2)*. Los Alamitos, CA, USA: IEEE Computer Society, nov 2022, pp. 10–19. [Online]. Available: <https://doi.ieeecomputersociety.org/10.1109/ESPM256814.2022.00007>
- [22] D. C. Marcelllo, S. Shiber, O. De Marco, J. Frank, G. C. Clayton, P. M. Motl, P. Diehl, and H. Kaiser, "octo-tiger: a new, 3D hydrodynamic code for stellar mergers that uses HPX parallelization," *Monthly Notices of the Royal Astronomical Society*, vol. 504, no. 4, pp. 5345–5382, 04 2021. [Online]. Available: <https://doi.org/10.1093/mnras/stab937>
- [23] S. Shiber, O. D. Marco, P. M. Motl, B. Munson, D. C. Marcelllo, J. Frank, P. Diehl, G. C. Clayton, B. N. Skinner, H. Kaiser, G. Daiss, D. Pflüger, and J. E. Staff, "Hydrodynamic simulations of WD-WD mergers and the origin of RCB stars," 2024.
- [24] P. Diehl, D. Marcelllo, P. Amini, H. Kaiser, S. Shiber, G. C. Clayton, J. Frank, G. Dais, D. Pflüger, D. Eder, A. Koniges, and K. Huck, "Performance Measurements Within Asynchronous Task-Based Runtime Systems: A Double White Dwarf Merger as an Application," *Computing in Science & Engineering*, vol. 23, no. 03, pp. 73–81, may 2021.
- [25] R. Tylenda, M. Hajduk, T. Kamiński, A. Udalski, I. Soszyński, M. K. Szymański, M. Kubiak, G. Pietrzyński, R. Poleski, L. Wyrzykowski, and K. Ulaczyk, "V1309 Scorpii: merger of a contact binary," *Astronomy & Astrophysics*, vol. 528, p. A114, Mar. 2011. [Online]. Available: <http://dx.doi.org/10.1051/0004-6361/201016221>
- [26] W. Even and J. E. Tohline, "CONSTRUCTING SYNCHRONOUSLY ROTATING DOUBLE WHITE DWARF BINARIES," *The Astrophysical Journal Supplement Series*, vol. 184, no. 2, p. 248, sep 2009. [Online]. Available: <https://dx.doi.org/10.1088/0067-0049/184/2/248>
- [27] R. Brooks and J. P. Matelski, "The dynamics of 2-generator subgroups of $psl(2, c)$," in *Riemann surfaces and related topics: Proceedings of the 1978 Stony Brook Conference*, vol. 1. Princeton University Press Princeton, New Jersey, 1981.
- [28] P. Diehl, S. R. Brandt, and H. Kaiser, "Shared Memory Parallelism in Modern C++ and HPX," *SN Computer Science*, vol. 5, no. 5, p. 459, Apr 2024. [Online]. Available: <https://doi.org/10.1007/s42979-024-02769-6>
- [29] P. Diehl and C. Taylor, "Shared memory parallelism in modern c++," <https://doi.org/10.5281/zenodo.8067170>, Jun. 2023.
- [30] P. Diehl, G. Daiß, K. Huck, D. Marcelllo, S. Shiber, H. Kaiser, and D. Pflüger, "Simulating Stellar Merger using HPX/Kokkos on A64FX on Supercomputer Fugaku," in *2023 IEEE International Parallel and Distributed Processing Symposium Workshops (IPDPSW)*. IEEE, 2023, pp. 682–691.
- [31] S. Sreepathi and M. Taylor, "Early Evaluation of Fugaku A64FX Architecture Using Climate Workloads," in *2021 IEEE International Conference on Cluster Computing (CLUSTER)*. IEEE, 2021, pp. 719–727.
- [32] R. E. Grant, M. Levenhagen, S. L. Olivier, D. DeBonis, K. T. Pedretti, and J. H. L. III, "Standardizing Power Monitoring and Control at Exascale," *Computer*, vol. 49, no. 10, pp. 38–46, Oct 2016.
- [33] Marcelllo, Shiber, and Diehl, "Restart data for the v1309 scenario," Aug. 2021. [Online]. Available: <https://doi.org/10.5281/zenodo.5213015>